Electronic Supplementary Material (ESI) for Catalysis Science & Technology.

Supplementary Information: Hydroxyapatite Supported Molybdenum Oxide Catalyst for Selective Oxidation of Methanol to Formaldehyde: Studies of Industrial Sized Catalyst Pellets

Joachim Thrane[1], Uffe Vie Mentzel[2], Max Thorhauge[2], Martin Høj[1], Anker Degn Jensen[1]*

[1] Department of Chemical and Biochemical Engineering, Technical University of Denmark (DTU), DK-2800 Kgs. Lyngby, Denmark.

[2] Haldor Topsøe A/S, DK-2800 Kgs. Lyngby, Denmark.

*aj@kt.dtu.dk

Contents

1 Pellet Impregnations

Table S1: Amounts of water, 30 wt% H_2O_2 in water and ammonium heptamolybdate used for the pellet impregnation solutions.

#	H_2O	30 wt% H_2O_2	$(NH_4)_6Mo_7O_{24}\cdot 4H_2O$
	[g]	[g]	[g]
2a	50.00	0.00	11.711
2b	9.06	3.00	5.787
3	7.70	2.52	4.556
4	7.69	2.56	3.151
5	7.69	2.57	2.569
6	7.69	2.56	2.495

2 Activity Tests

2.1 Test criteria for lab scale powder measurements

To ensure that the results obtained during activity measurements were reliable a number of different criteria have been evaluated to estimate whether the data may be expected to be influenced by flow bypass from a bad bed design or mass and heat transport limitations. In the following, the criteria will be given.

2.1.1 Design criteria for PBR

For a PBR it has been found empirically that the particle size to tube ratio should be above 10 (Equation (S1)) to ensure close to ideal reactor plug flow behavior as the packing density at the tube wall is lower which may give higher local velocities due to increased voidage.

$$\frac{d_{tube}}{d_p} > 10 \tag{S1}$$

A criterion was developed by Gierman and Mears (Equations (S2)-(S3)) for the catalyst bed length necessary to neglect the effect of axial dispersion/diffusion and get behavior close to an ideal PBR [1].

$$L_{bed} > \frac{8nd_p}{Pe_p} ln\left(\frac{1}{1-X}\right) \tag{S2}$$

$$Pe_p = \frac{L_B u}{D_{Ax}} \tag{S3}$$

Where, L_B was the length of the catalyst bed, n reaction order and Pe_p was the particle Peclet number (0.3-0.7 in laboratory reactors [1]), D_{Ax} the axial dispersion coefficient, u the superficial velocity.

To decrease the temperature gradient, and increase the length of the catalyst bed, the catalyst sample was diluted with SiC. The influence of dilution is described by two criteria for a deviation of maximum 5% for either the conversion (Equation (S4)) or the calculated 1st order rate constant (Equation (S5)) [1], [2].

$$\Delta \equiv \frac{X_{undiluted}-X_{diluted}}{X_{undiluted}} \approx \frac{b}{1-b}\frac{nXd_p}{2L_B} = \frac{bnXd_p}{2L_0} < 0.05 \tag{S4}$$

$$\Delta_k \equiv \frac{k_{undiluted}-k_{diluted}}{k_{undiluted}} = \frac{ln\left(\frac{1-X(1-\Delta)}{1-X}\right)}{ln\left(\frac{1}{1-X}\right)} < 0.05 \tag{S5}$$

Where X is the conversion, b the volumetric dilution, L_0 bed length with no dilution and k the reaction rate constant. Due to the logarithmic nature of the calculation of the rate constant $\Delta_k > \Delta$.

2.1.2 Mass and heat transport limitations

2.1.2.1 Intra and extra particle gradients

For external particle mass transfer limitations the Carberry criterion (Equation (S6)) can be evaluated [1].

$$\mathrm{Ca} = \frac{-r_{obs}\rho_{cat}}{k_f(S/V)c_b} < 0.05 \qquad \text{(S6)}$$

Where r_{obs} is the mass based reaction rate, k_f the mass transfer coefficient in the fluid, V particle volume, S external surface area, c_b bulk reactant concentration, ρ_{cat} the catalyst density.

For extra particle heat transport an analogue to the Carberry criterion can be used [1] (Equation (S7)).

$$\frac{E_a}{R_g T_{bulk}} \frac{(-\Delta H_r)k_f c_b}{h_f T_{bulk}} \mathrm{Ca} < 0.05 \qquad \text{(S7)}$$

Where ΔH_r is the reaction enthalpy, h_f the heat transfer coefficient in the fluid, and T_{bulk} the temperature of the gas in the bulk. h_f and k_f were calculated by the analogues equations valid for $3<Re_p<2000$ shown for h in Equations (S8)-(S10).

$$h_f = \frac{0.357}{\epsilon_b} Re_p^{0.641} Pr^{1/3} \frac{\lambda_f}{d_p} \qquad \text{(S8)}$$

$$Re_p = \frac{\rho_f u d_p}{\mu_f} \qquad \text{(S9)}$$

$$Pr = \frac{\mu_f \hat{C}_{pf}}{\lambda_f} \qquad \text{(S10)}$$

Where Re_p was the particle Reynolds number, ϵ_b the bed porosity, ρ_f fluid density, μ_f dynamic viscosity of fluid, Pr the Prandtl number, $\hat{C}_{pf}$ mass heat capacity of fluid, λ_f heat conductivity of fluid. Alternatively, to the criteria, the temperature difference over the film can be calculated directly from Equation (S11) if the reaction rate is known.

$$\Delta T = \frac{-r_{obs}\rho_{cat}V(-\Delta H_r)}{h\,S} \qquad \text{(S11)}$$

For intra particle mass transfer limitations the Weisz-Prater criterion (Equation (S12))[3] is applicable.

$$\mathrm{C}_{\mathrm{WP}} = \frac{(-r_{obs})\rho_{cat}R^2}{D_e c_s} < 1 \qquad \text{(S12)}$$

Where c_s is the surface concentration, R the particle radius and D_e is the effective diffusion coefficient. For intra particle heat transport an analogue to the Wheeler-Weisz [1] criterion can be used (Equation (S13)).

$$\frac{E_a}{R_g T_s} \frac{(-\Delta H_r)k_f c_s}{h_c T_s} \Phi < 0.1 \qquad \text{(S13)}$$

Where T_s is the surface temperature and h_c is the heat transfer coefficient in the catalyst particle.

Alternatively, as the effective diffusion coefficient was estimated from the Hg-porosimetry measurements, the effectiveness factor can be estimated using Equations (6)-(8) from the main article to indicate the level of internal mass transfer limitations.

2.1.2.2 Bed gradients

For the temperature effects in the catalyst bed, Mears developed a criterion for the average reaction rate over the whole cross-section of a PBR (Equations (S14)-(S15)) [1], [4].

$$\frac{E_a}{RT_w}\left|\frac{(-r_{obs})\rho_{cat}(1-\epsilon_b)(1-b)(-\Delta H_r)d_{tube}^2}{4\lambda_{b,eff}T_w}\right|\left(\frac{1}{8}+\frac{1}{Bi_{h,w}}\frac{d_p}{d_{tube}}\right) < 0.05 \tag{S14}$$

$$Bi_{h,w} = \frac{h_w d_p}{\lambda_{b,eff}} \tag{S15}$$

Where T_w is the wall temperature, $\lambda_{b,eff}$ the effective heat conductivity, $Bi_{h,w}$ the wall Biot number and h_w the wall heat transfer coefficient.

Experimentally, the difference between the measured oven temperatures (two different thermocouples) and the measured reactor temperature may indicate the temperature difference throughout the bed.

2.1.3 Evaluation of criteria

The particle size to tube size criterion (Equation (S1)) states that the particles should be smaller than 400 µm as the reactor tube has 4 mm inner diameter. Since the bed length was at least 10 mm there was no influence until 95% conversion (Table S2), which was only exceeded at 400°C for measurements on powdered catalyst (#4, #5 and #6).

Table S2: Length of catalyst bed necessary to have close to ideal PFR behavior and negligible axial dispersion effect. Evaluated from Equation (S2).

***X* [%]**	1	10	30	50	70	90	95	99
***L_B* [mm]**	0.0	0.3	1.1	2.2	3.9	7.4	9.6	14.7

The dilution effect on the uncertainty due to the possibility of by-pass was evaluated (Figure S1).

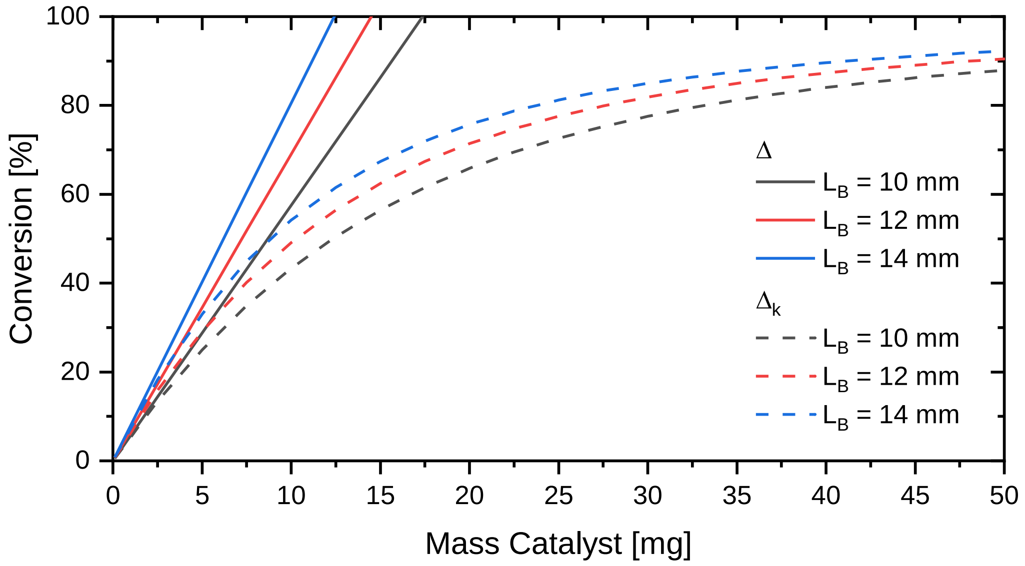

Figure S1: Evaluation of dilution criteria (Equations (S4) and (S5)) w.r.t. 5% deviation on the measured conversion (Δ) and the calculated 1st order reaction constant (Δ_k), when diluted with 150 mg SiC.

With 25 mg catalyst, the conversion would not have 5% uncertainty at any conversions, but the reaction rate constant would exceed 5% uncertainty above 70% conversion.

The heat and mass transfer criteria, were evaluated for the #6 pellet ($\rho = 1.18$ g/cm^3) powder test (Table S3) indicating an effect of external heat transfer limitations from 350°C and above (estimated maximum of 6 K difference) and internal mass transfer limitations from 350°C and above. According to the criterion (Equation (S14)) the temperature gradient in the bed, will influence the measurements from 300°C. As an indication of the maximum possible temperature difference over the bed, the difference between the thermocouples on the inside of the heating oven and the thermocouple touching the top of the catalyst bed, can be used. At low conversions/no reaction, especially one of the oven thermocouples measured very similar to the reactor thermocouple and was thus preferential to use. The difference increased with increasing conversion. Thus the maximum difference in temperature over the catalyst bed was 23.6 K at 400°C for the powdered #6 pellet (Table S3).

Table S3: Evaluation of transport criteria for performed the #6 pellet powder test results. The effectiveness factor using Equation (6) in the main manuscript, the temperature difference over the stagnant film, and the measured temperature difference (ΔT_{max}) between the most similar oven thermocouple (with no reaction) and the reactor thermocouple touching the top of the bed as a measure of maximum possible bed temperature difference.

		Criterion	Eq.	Limit	250°C	300°C	350°C	400°C
Extra particle	Mass	Carberry	(S6)	<0.05	0.001	0.006	0.026	0.052
	Heat	Carberry	(S7)	<0.05	0.008	0.038	0.111	0.143
		ΔT [K]	(S11)		0.2	1.0	3.6	5.5
Intra particle	Mass	Weisz-Prater	(S12)	<1	0.033	0.206	1.038	2.174
		η			0.998	0.985	0.927	0.770
	Heat	Wheeler-Weisz	(S13)	<0.1	0.000	0.001	0.003	0.003
Estimated maximum axial temperature bed gradient	Heat	Mears	(S14)	<0.05	0.017	0.076	0.216	0.273
		ΔT_{max} [K]			2.2	7.6	22.4	23.6

2.2 Single pellet experiments

For the single pellet experiments it is of interest to know how external mass and heat transport limitations may affect the measurements. The random pore model was used to obtain the effective diffusion coefficient and calculate the internal mass transport limitations (effectiveness factor). This was done by treating the single pellet as a single spherical particle, and reusing the Carberry criteria (Equations (S6) and (S7)) (Where D_h was the hydraulic diameter, Gz the Graetz number and L_{pellet} the length of the catalyst pellet.

Table S4), where the heat and mass transfer were calculated by analogues equations (Equations (S16)-(S18)).

$$h = \frac{Nu \cdot \lambda_f}{V/S} \tag{S16}$$

$$Nu = 3.66 + \frac{0.085\ Gz}{1+0.047\ Gz^{\frac{2}{3}}} \tag{S17}$$

$$Gz = Re\ Pr \frac{D_h}{L_{pellet}} \tag{S18}$$

Where D_h was the hydraulic diameter, Gz the Graetz number and L_{pellet} the length of the catalyst pellet.

Table S4: Evaluation of external mass and heat transport criteria for the #6 ($\rho = 1.18$ g/cm^3) pellet from the experimental results on a single pellet and an estimate of the overall influence on measured rate.

	Criterion	Eq.	Limit	250°C	300°C	350°C	400°C
Mass	Carberry	(S6)	<0.05	0.014	0.070	0.152	0.223
Heat	Carberry	(S7)	<0.05	0.038	0.156	0.286	0.358
	ΔT [K]	(S11)		1.3	6.5	14.0	20.6

The external mass and heat transport was found by the evaluation of the Carberry criteria for the pellet to have significant influence at 300°C and higher temperatures (Where Dh was the hydraulic diameter, Gz the Graetz number and L_{pellet} the length of the catalyst pellet.

Table S4) and could thus not be neglected.

3 MoO$_3$ evaporation setup

The setup used for the MoO$_3$ evaporation investigations were the same setup as described in [5] (

Figure S2 and Figure S3).

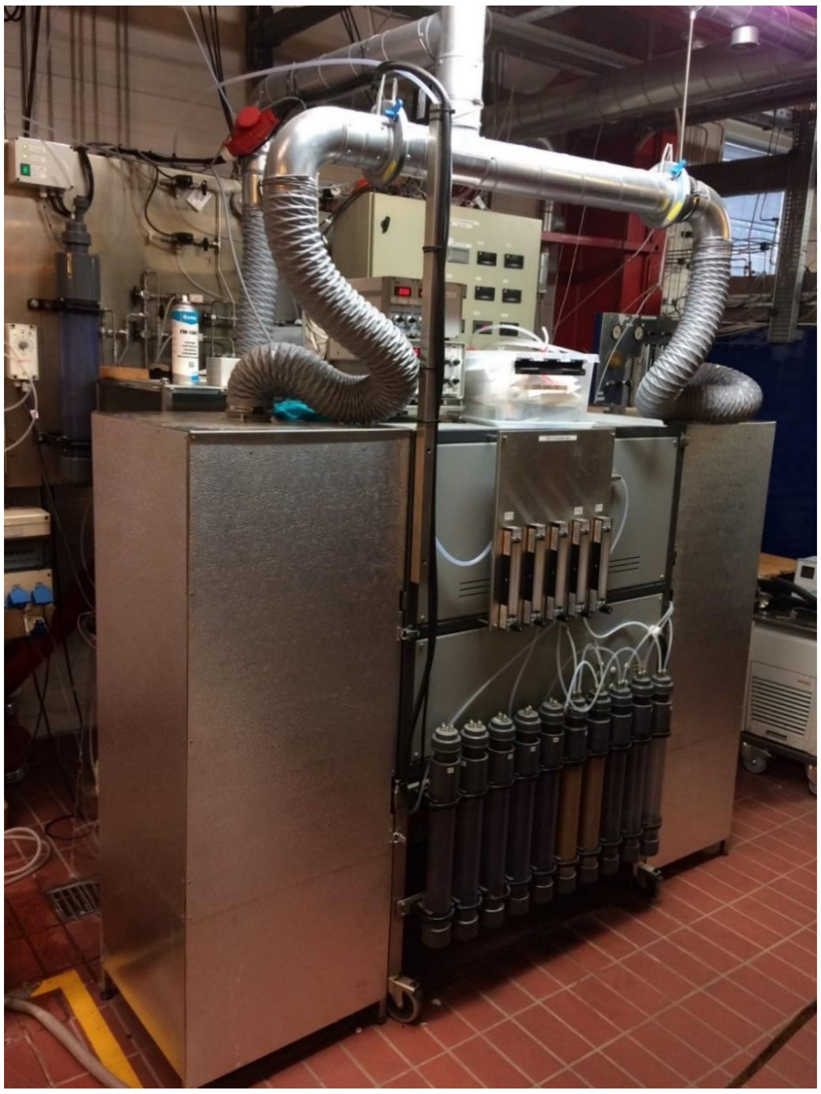

Figure S2: Picture showing the setup used for Mo evaporation measurements.

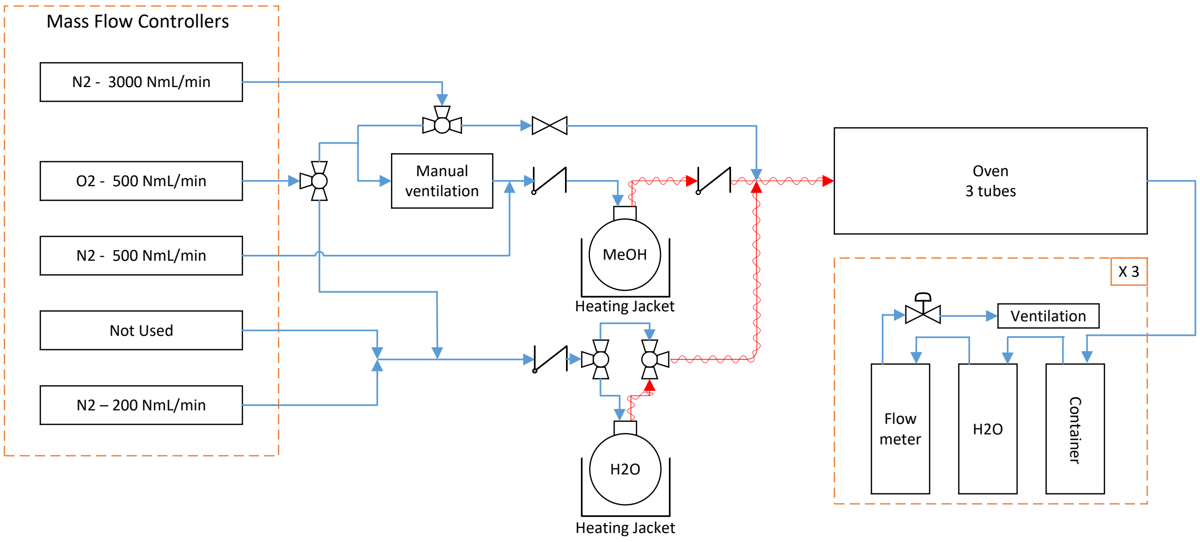

Figure S3: P & I diagram for the setup used for the Mo evaporation investigations.

4 XRD

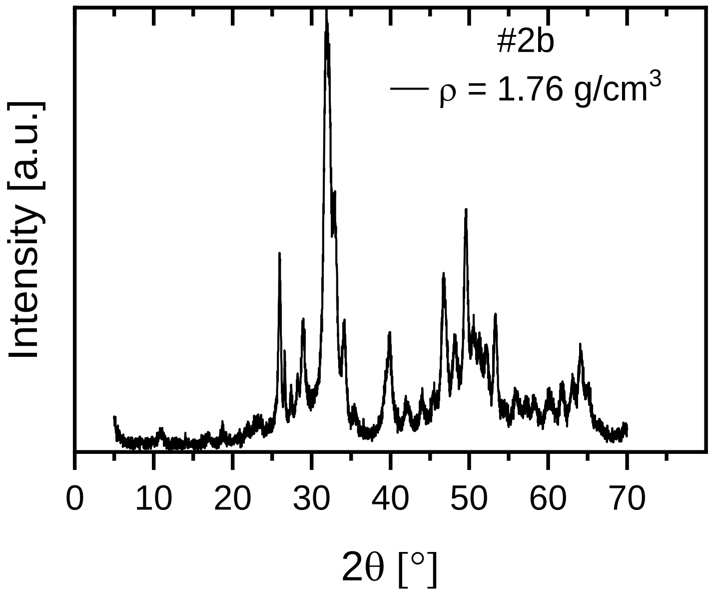

Figure S4: XRD diffractogram of fresh catalyst sample ρ = 1.76 g/cm^3 (#2b).

5 Pellet mass loss

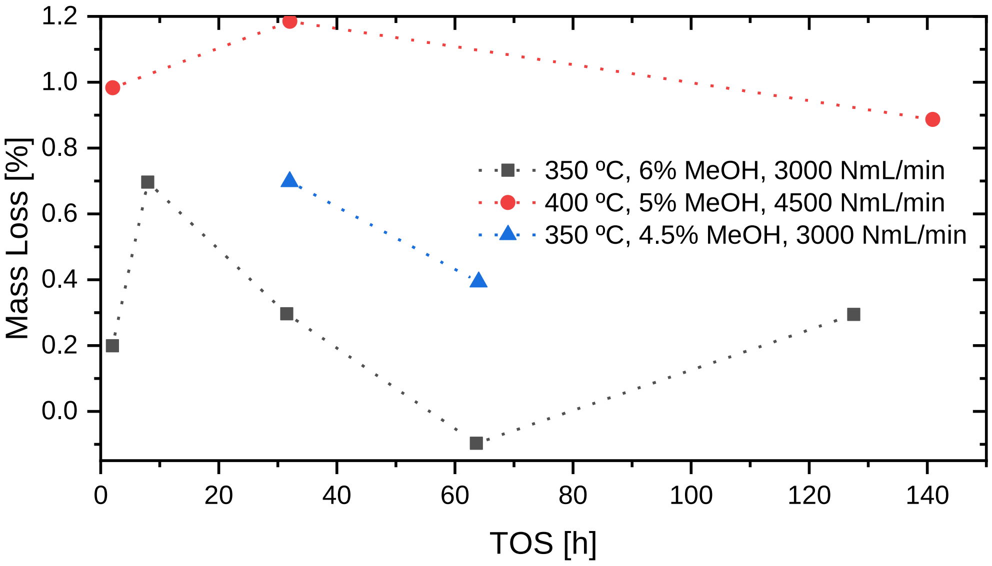

Figure S5: Mass loss from 100 mg pellets during exposure to reactions conditions. The error bars on TOS was due to uncertainty of reactor breakage giving a total loss of flow.

6 SEM

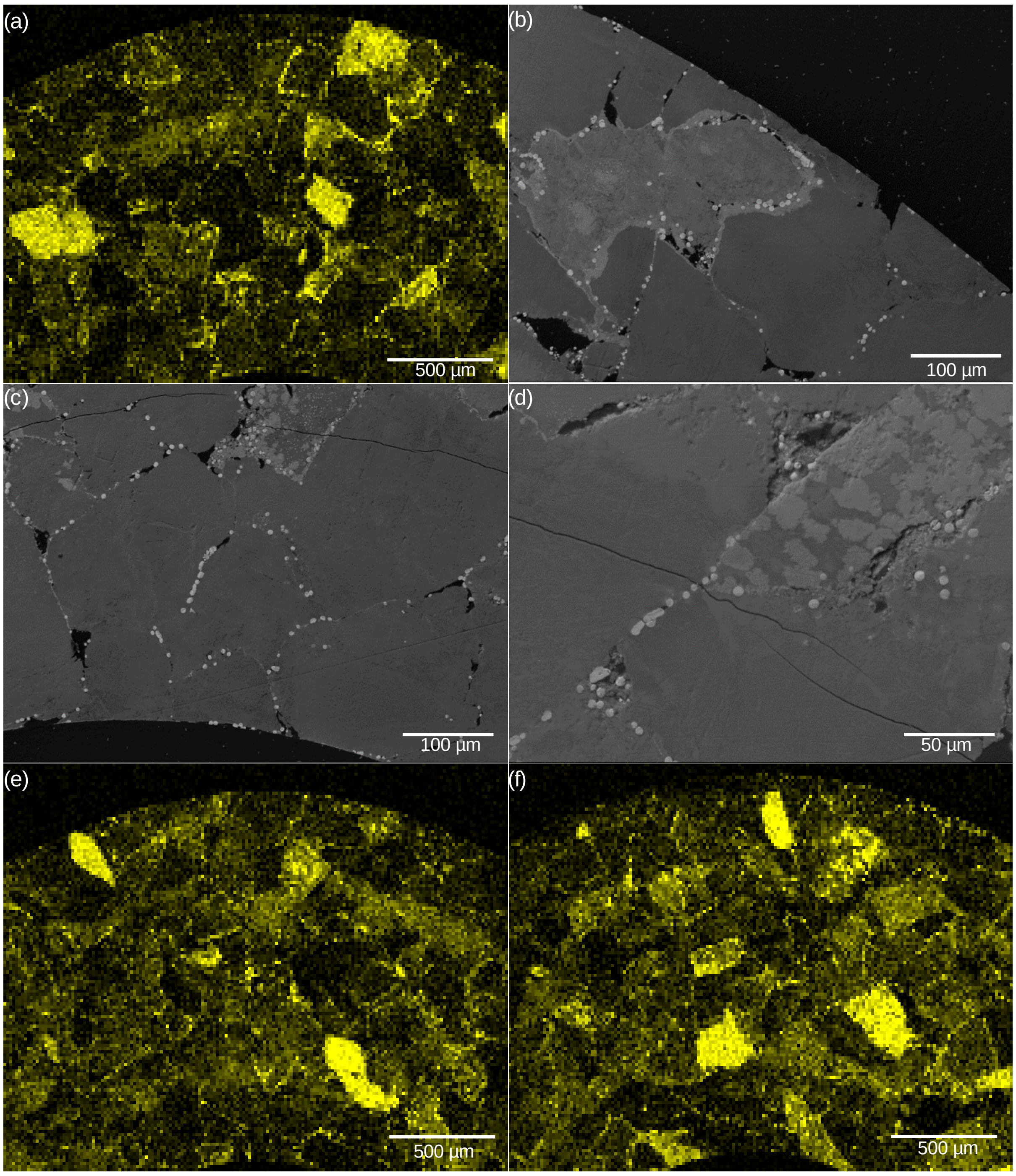

Figure S6: SEM images and EDX maps of the catalyst sample with ρ = 1.84 g/cm^3 fresh and after exposure experiment. (a) fresh whole cross section of cylinder wall, (b) fresh pellet cross section near outer surface, (c) fresh pellet cross section near inner surface, (d) close up cross section middle of cylinder wall, (e) 141 h at 400°C spent pellet, (f) 64 h at 350°C spent pellet.

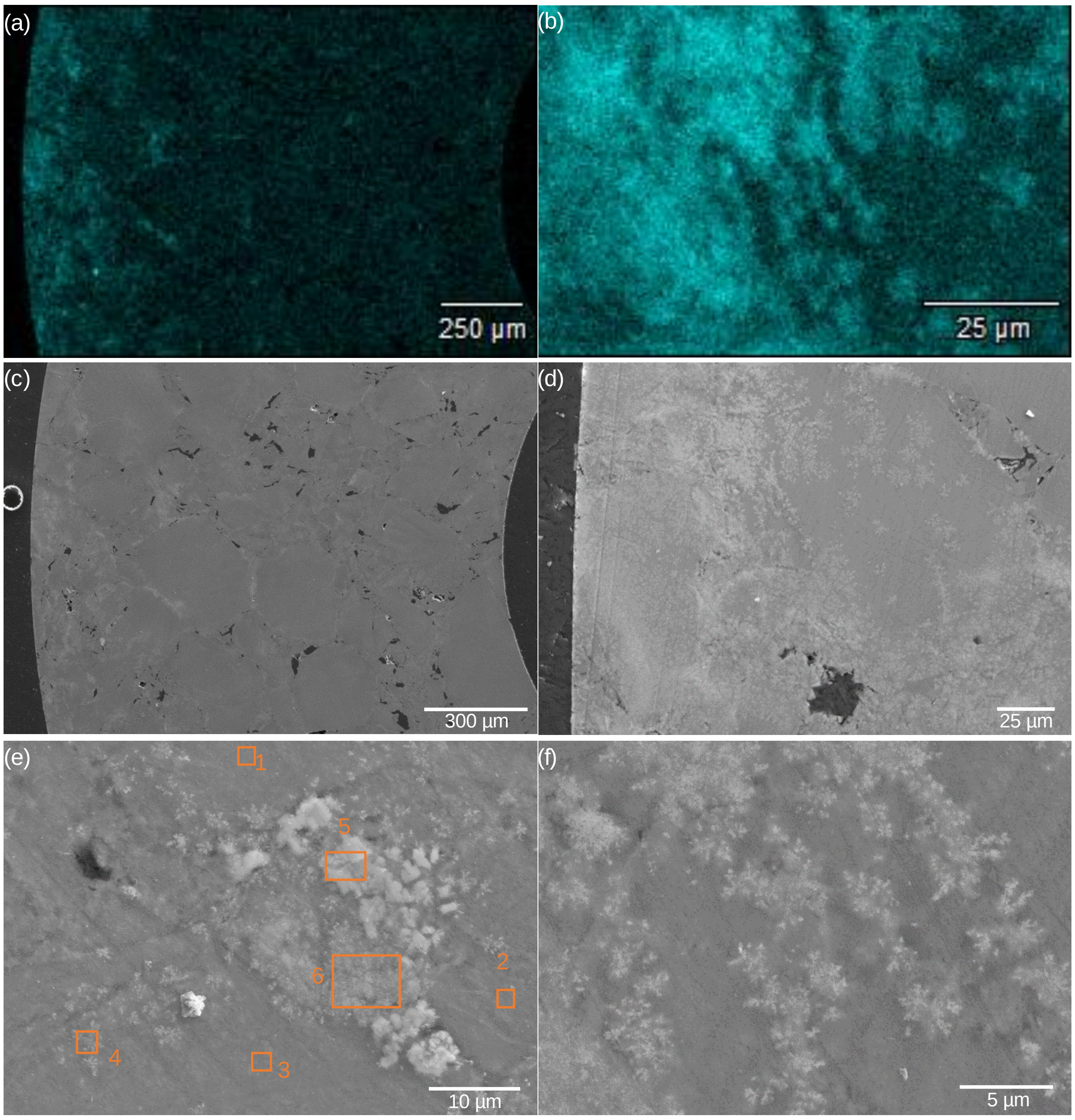

Figure S7: SEM images and EDX maps of the catalyst sample with ρ = 1.76 g/cm^3 fresh (#2a). (a) EDX map cross section of whole pellet wall, (b) EDX map cross section middle of pellet wall, (c) cross section whole pellet wall, (d) close up pellet cross section near outer surface, (e) close up Mo rich ensamples, (f) close up Mo rich ensamples. EDX measurements: 1: Ca/P = 1.63, 9.2 wt% MoO_3, 2: Ca/P = 1.63, 8.9 wt% MoO_3, 3: Ca/P = 1.65, 8.4 wt% MoO_3, 4: Ca/P = 1.65, 15.0 wt% MoO_3, 5: Ca/P = 2.33, 38.1 wt% MoO_3, 6: Ca/P = 1.72, 23.1 wt% MoO_3.

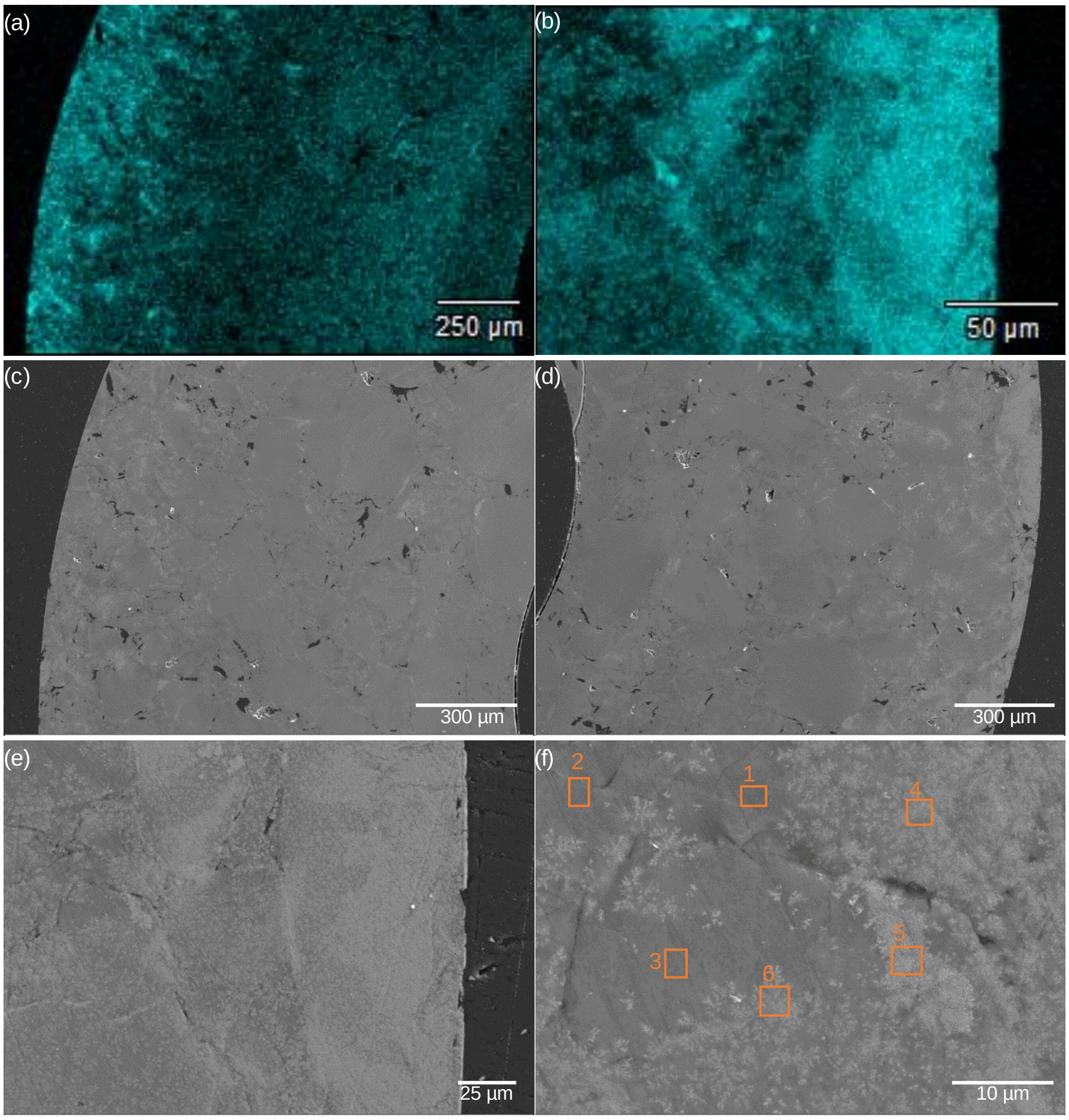

Figure S8: SEM images and EDX maps from cross sections of catalyst sample with ρ = 1.76 g/cm^3 fresh (#2b). (a) EDX map whole pellet wall, (b) EDX map close to outer surface, (c) whole pellet wall, (d) opposite side whole pellet wall, (e) close up near outer surface, (f) close up Mo rich ensamples. EDX measurements: 1: Ca/P = 1.65, 7.8 wt% MoO_3, 2: Ca/P = 1.67, 8.0 wt% MoO_3, 3: Ca/P = 1.65, 8.7 wt% MoO_3, 4: Ca/P = 1.64, 26.1 wt% MoO_3, 5: Ca/P = 1.71, 34.8 wt% MoO_3, 6: Ca/P = 1.68, 21.0 wt% MoO_3.

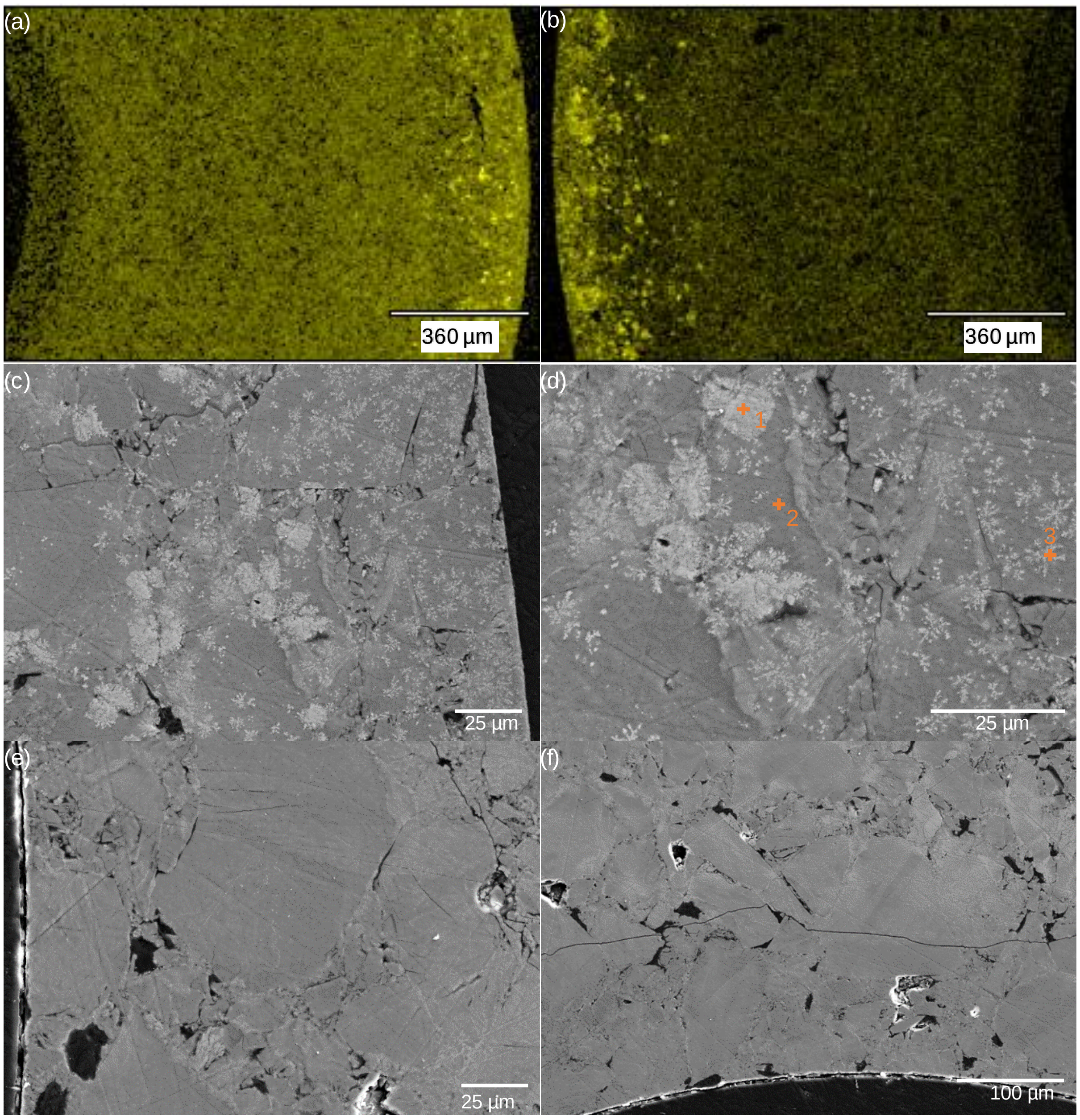

Figure S9: SEM images and EDX maps on cross section of catalyst sample with ρ = 1.59 g/cm^3 after 118.5 h of exposure experiment. (a) EDX Map whole pellet wall, (b) EDX map opposite pellet wall, (c) close up near pellet outer surface, (d) close up on part of (c), (e) close up near pellet inner surface, (f) close up near pellet inner surface. EDX measurements: 1: Ca/P = 1.65, 36.9 wt% MoO_3, 2: Ca/P = 1.65, 13.2 wt% MoO_3, 3: Ca/P = 1.74, 24.8 wt% MoO_3.

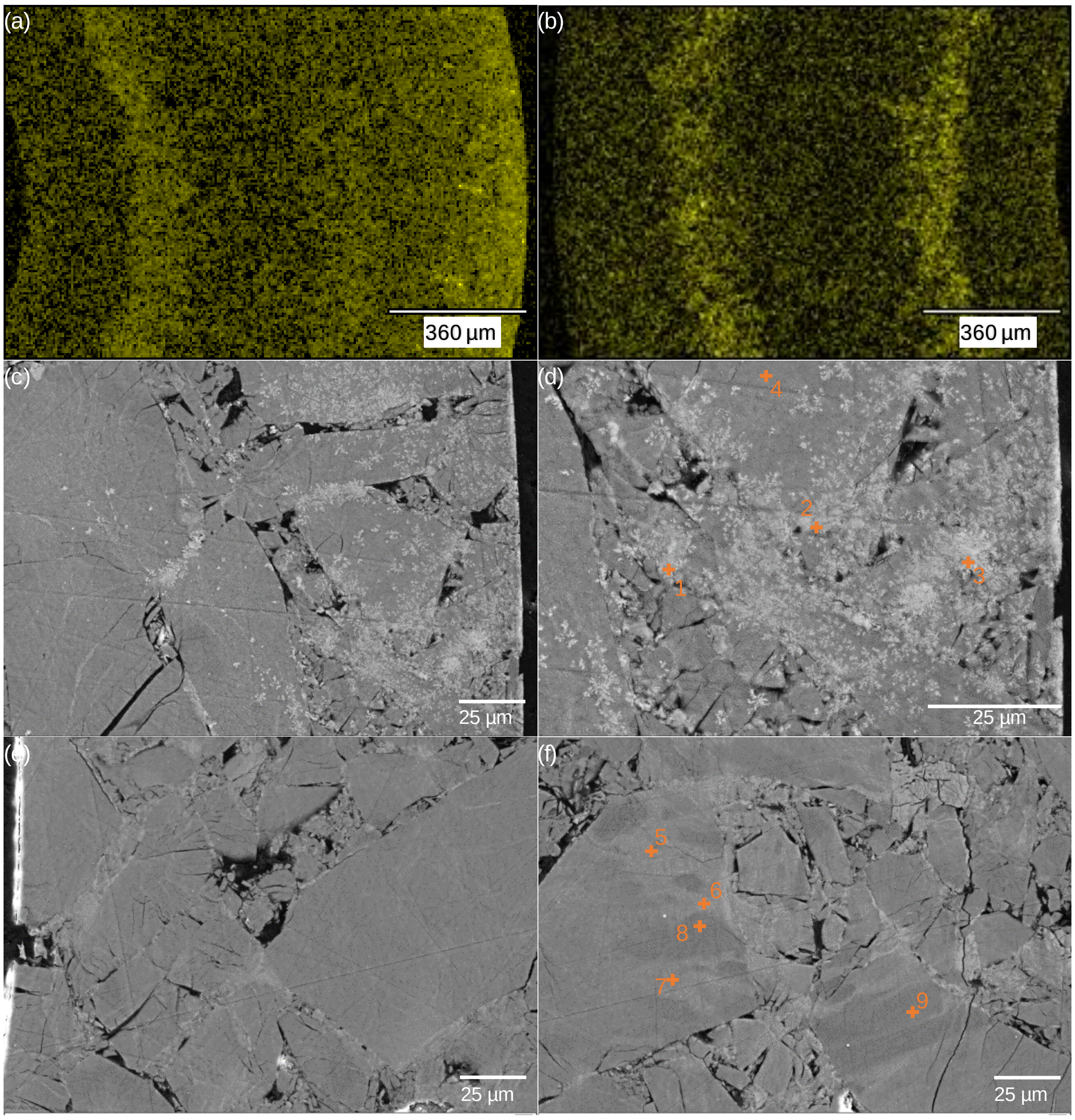

Figure S10: SEM images and EDX maps on cross section of catalyst sample with $\rho = 1.44$ g/cm^3 after 118.5 h of exposure experiment. (a) EDX map pellet cylinder wall, (b) EDX map opposite pellet cylinder wall, (c) SEM image near outer surface, (d) SEM close up near outer surface, (e) SEM image near outer surface, (f) SEM image middle of pellet. 1: Ca/P = 1.62, 21.8 wt% MoO$_3$, 2: Ca/P = 1.64, 18.2 wt% MoO$_3$, 3: Ca/P = 1.59, 34.5 wt% MoO$_3$, 4: Ca/P = 1.63, 10.4 wt% MoO$_3$, 5: Ca/P = 1.72, 15.6 wt% MoO$_3$, 6: Ca/P = 1.72, 15.6 wt% MoO$_3$, 7: Ca/P = 1.78, 11.6 wt% MoO$_3$, 8: Ca/P = 1.93, 4.2 wt% MoO$_3$, 10: Ca/P = 1.90, 4.7 wt% MoO$_3$,.

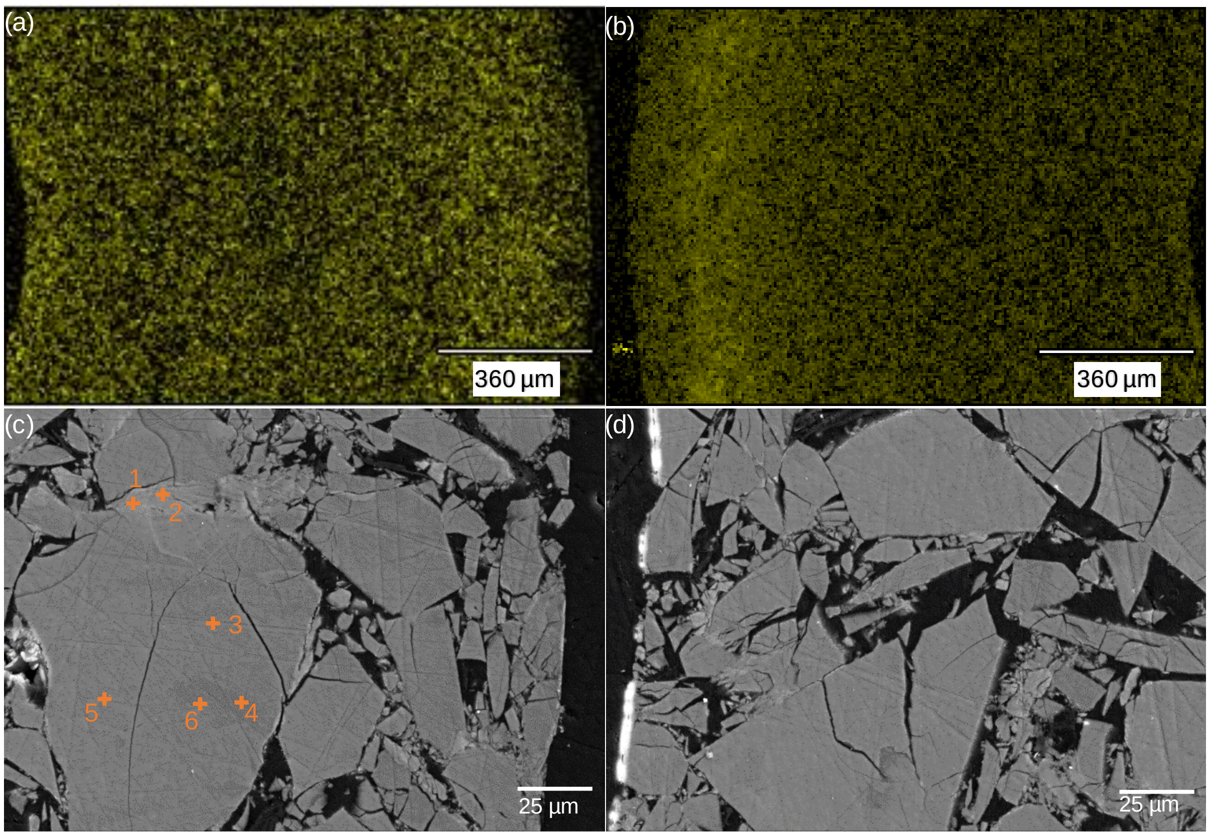

Figure S11: SEM images and EDX maps from cross section of catalyst sample with ρ = 1.26 g/cm^3 after 118.5 h of exposure experiment (a) EDX map pellet cylinder wall, (b) EDX map opposite pellet cylinder wall, (c) SEM image near outer surface, (d) SEM close up near outer surface,. EDX measurements: 1: Ca/P = 1.61, 8.1 wt% MoO_3, 2: Ca/P = 1.63, 8.1 wt% MoO_3, 3: Ca/P = 1.95, 8.4 wt% MoO_3, 4: Ca/P = 1.81, 6.2 wt% MoO_3, 5: Ca/P = 1.84, 9.3 wt% MoO_3, 6: Ca/P = 1.87, 6.6 wt% MoO_3.

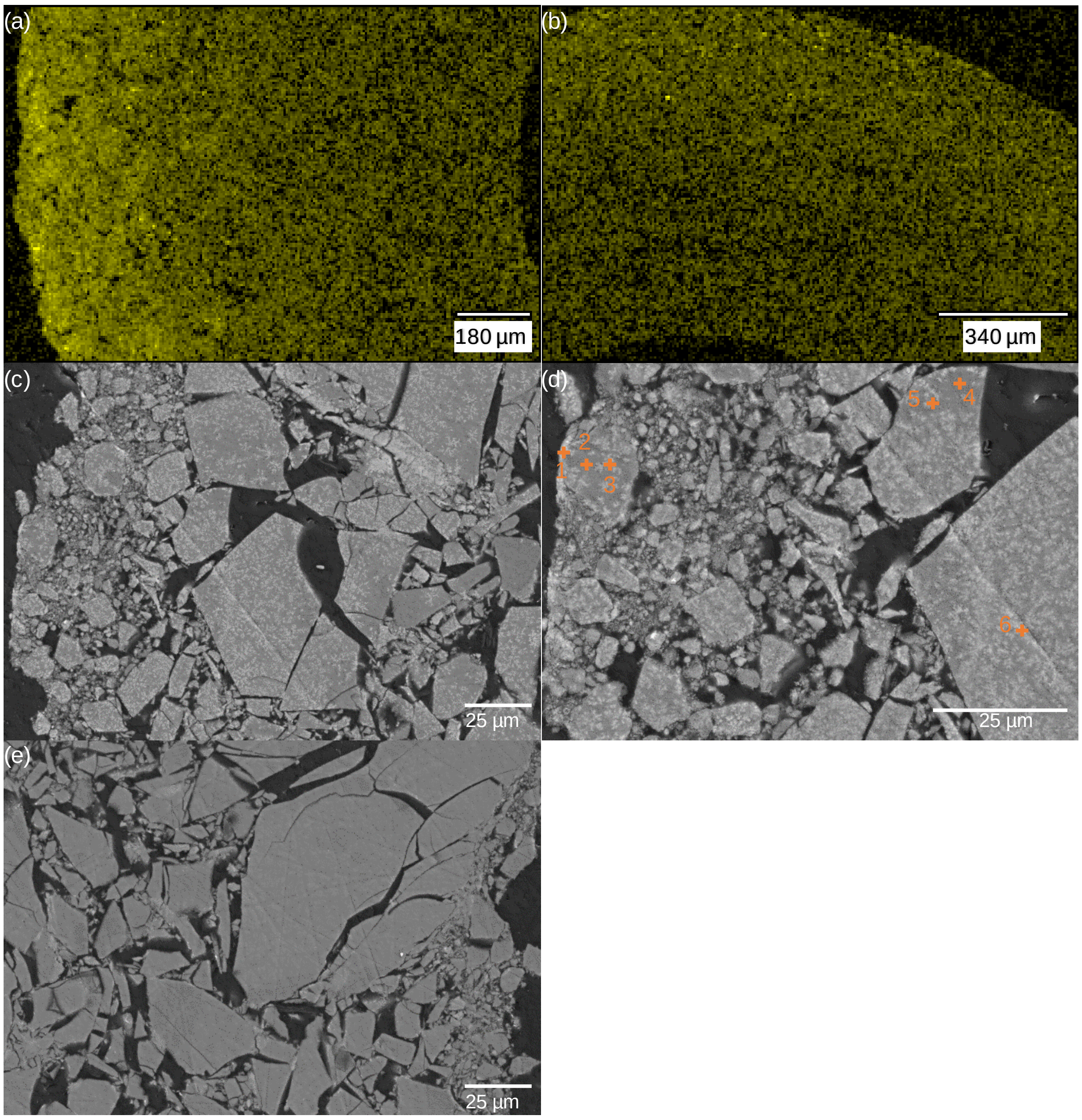

Figure S12: SEM images and EDX maps of cross section of catalyst sample with ρ = 1.18 g/cm^3 after 118.5 h of exposure experiment. (a) EDX map whole cylinder wall, (b) EDX map other part of cylinder wall, (c) SEM close up near outer surface, (d) SEM closer close up outer surface, (e) SEM close up middle of pellet. 1: Ca/P = 1.75, 23.7 wt% MoO_3, 2: Ca/P = 1.66, 9.6 wt% MoO_3, 3: Ca/P = 1.70, 22.8 wt% MoO_3, 4: Ca/P = 1.62, 9.0 wt% MoO_3, 5: Ca/P = 1.70, 21.5 wt% MoO_3, 6: Ca/P = 1.67, 24.3 wt% MoO_3.

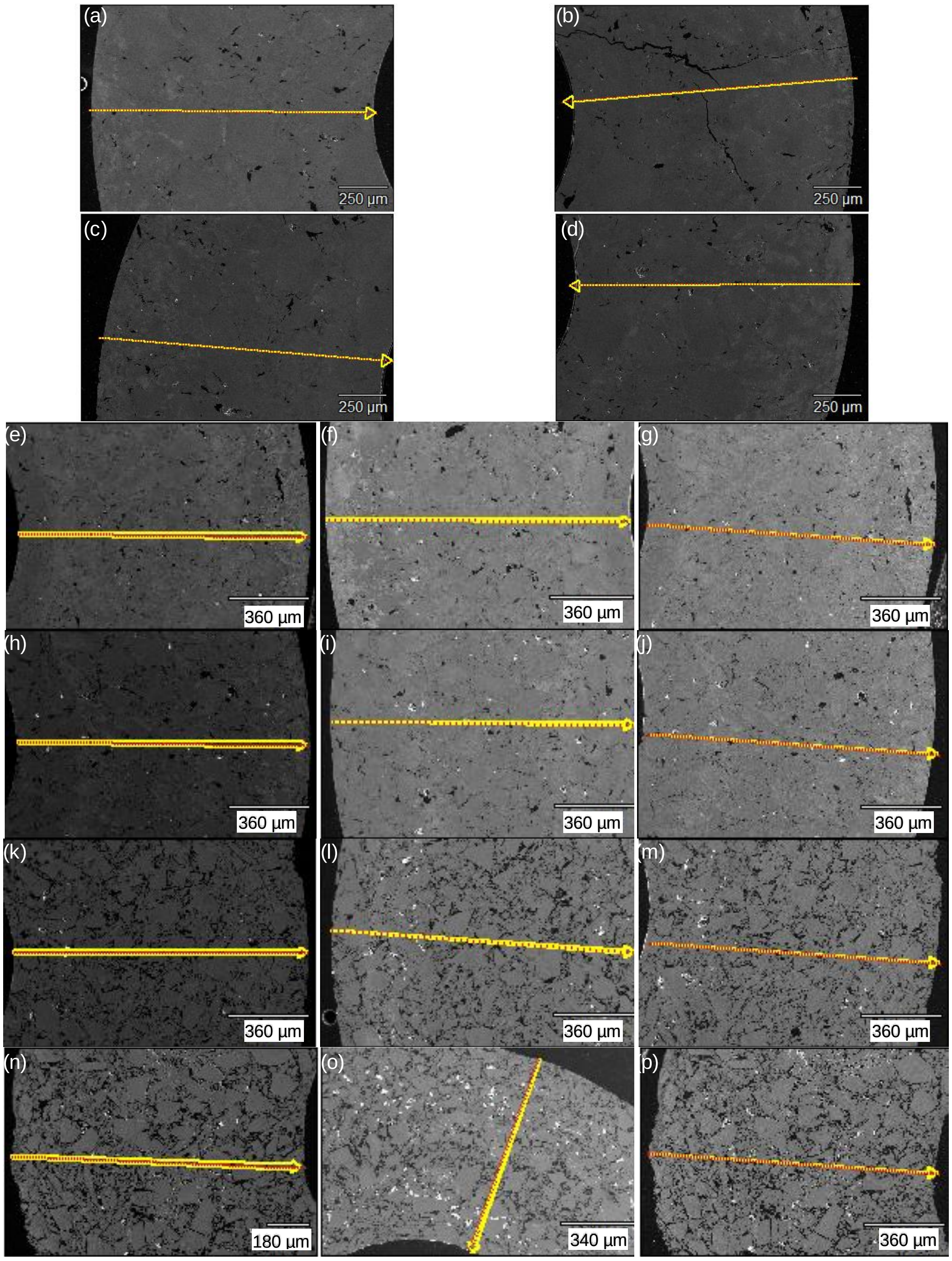

Figure S13: SEM images and lines showing where on the cross section the SEM EDX map extractions and line scans were performed. #2a: line scan 1 (a), line scan 2 (b), #2b: line scan 1 (c), line scan 2 (d), #3: map extract 1 (e), map extract 2 (f), line scan (g), #4: map extract 1 (h), map extract (i), line scan (j), #5: map extract 1 (k), map extract 2 (l), line scan (m), #6: map extract 1 (n), map extract 2 (o), line scan (p).

6.1 Arrhenius plots

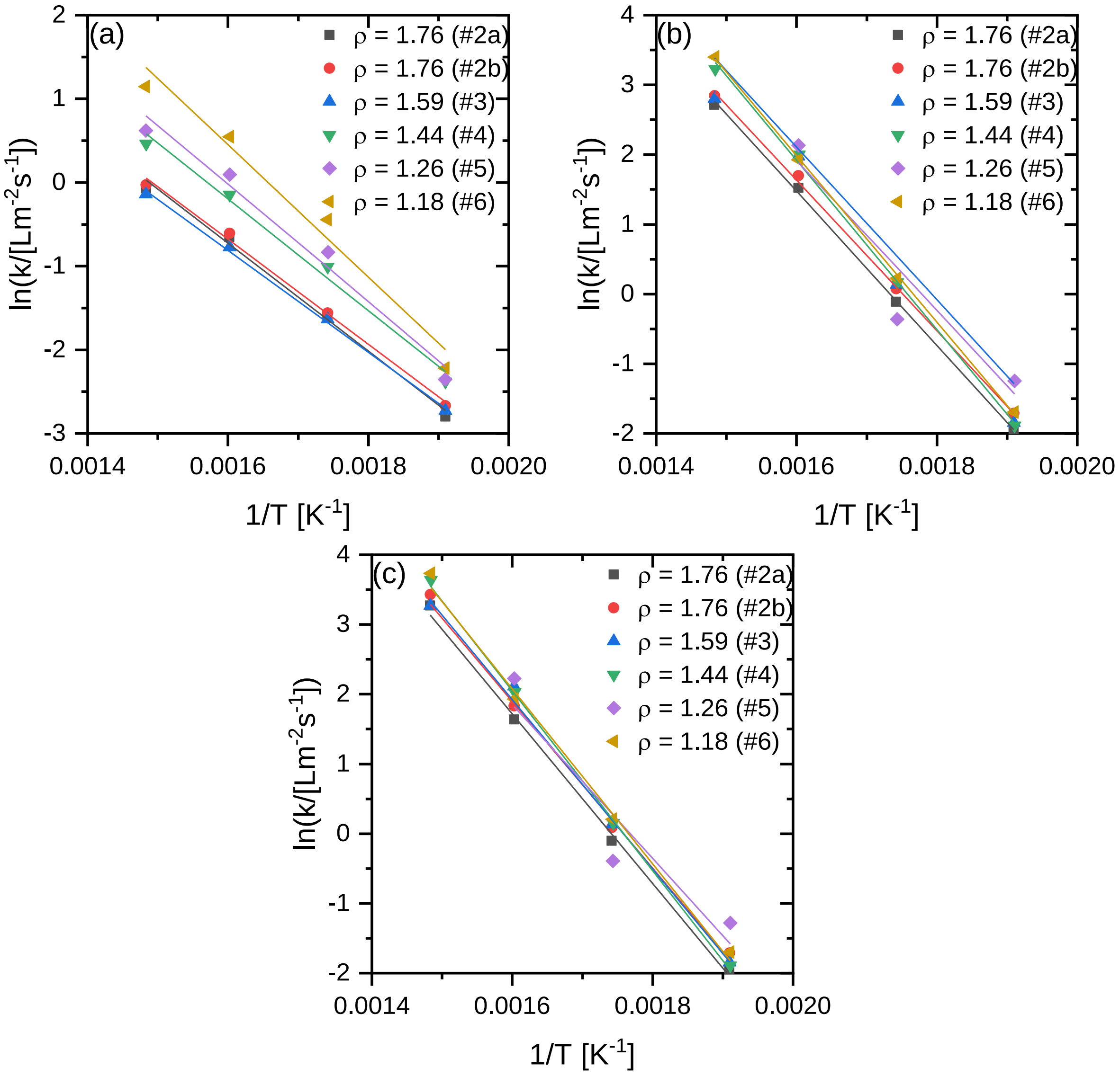

Figure S14: Arrhenius plot for: (a) impregnated catalyst pellets; (b) pellets crushed to powder; (c) the intrinsic activity calculated from the powder, taking into account the overall effectiveness factor and external heat transfer limitations (c).

6.2 Effectiveness factors and intrinsic rate

In the calculations of the effectiveness factors and the intrinsic rate constant, the catalyst particles and pellets have been assumed isothermal. The catalyst bed has been assumed to be isothermal at the temperature measured at the top of the catalyst bed, and behave as an ideal PBR.

Table S5: Intrinsic rate constant calculated from powder measurements using Equation (9) taking into account the internal and external diffusion (Table S6) and the temperature difference over the gas film to the powder (Table S7). The bed temperature is assumed isothermal and equal to that measured by the thermocouple.

#	ρ_{target}	250°C	300°C	350°C	400°C
	[g/cm^3]	[L/kg/s]	[L/kg/s]	[L/kg/s]	[L/kg/s]
1	1.84	3.7	24.9	125.9	516.1
2a	1.76	3.9	25.3	143.1	726.9
2b	1.76	4.6	27.5	156.3	765.2
3	1.59	4.9	35.7	255.8	810.9
4	1.44	4.7	36.2	234.7	1173.9
5	1.26	12.9	31.3	426.7	nd
6	1.18	5.7	38.5	214.3	1301.0

Table S6: Internal and overall effectiveness factor calculated for the powder measurements using Equations (6) and (7) at the powder temperature (thermocouple measurement plus *ΔT* from Table S7).

#	ρ_{target}	Ω				η			
		250°C	**300°C**	**350°C**	**400°C**	**250°C**	**300°C**	**350°C**	**400°C**
	[g/cm^3]	**[%]**	**[%]**	**[%]**	**[%]**	**[%]**	**[%]**	**[%]**	**[%]**
1	1.84	99.5	96.7	85.6	62.1	99.6	97.3	87.8	66.9
2a	1.76	99.2	95.4	79.1	48.1	99.3	95.9	81.3	52.5
2b	1.76	99.1	95.0	77.7	47.2	99.2	95.6	80.1	51.6
3	1.59	99.3	95.4	75.0	53.0	99.4	96.2	78.5	58.4
4	1.44	99.6	97.2	84.4	56.0	99.7	97.9	87.8	63.7
5	1.26	99.2	98.2	80.5	nd	99.4	98.7	84.9	nd
6	1.18	99.7	98.0	90.1	63.0	99.8	98.6	92.7	70.9

Table S7: Temperature difference over gas film for powder and pellet measurements calculated by Equation (S11) used for calculating the powder and pellet temperatures.

#	ρ_{target}	Powder				Pellets			
		250°C	**300°C**	**350°C**	**400°C**	**250°C**	**300°C**	**350°C**	**400°C**
	[g/cm^3]	**[K]**	**[K]**	**[K]**	**[K]**	**[K]**	**[K]**	**[K]**	**[K]**
1	1.84	0.2	1.1	3.8	6.8	0.7	2.2	4.8	-
2a	1.76	0.2	1.2	4.2	7.2	0.9	2.5	5.4	8.3
2b	1.76	0.2	1.2	4.2	7.1	0.9	2.4	5.2	8.0
3	1.59	0.2	1.3	5.1	6.8	0.9	2.4	4.9	8.0
4	1.44	0.2	1.2	4.5	6.4	1.1	3.8	7.6	11.7
5	1.26	1.1	1.4	4.6	5.1	1.5	5.7	11.7	16.3
6	1.18	0.2	0.9	3.3	4.9	1.0	5.0	11.0	16.2

Table S8: Internal and overall effectiveness factor calculated for the pellet measurements using Equations (6) and (7) with the intrinsic rate constant (Table S5) corrected to the pellet temperature (thermocouple measurement plus ΔT from Table S7) using the intrinsic activations energy (Table 6).

#	ρ_{target}	Ω				η			
		250°C	**300°C**	**350°C**	**400°C**	**250°C**	**300°C**	**350°C**	**400°C**
	[g/cm^3]	**[%]**	**[%]**	**[%]**	**[%]**	**[%]**	**[%]**	**[%]**	**[%]**
1	1.84	55.9	25.9	11.9	6.4	56.2	26.3	12.3	6.8
2a	1.76	47.4	21.4	9.1	4.0	47.6	21.6	9.4	4.3
2b	1.76	44.8	20.6	8.8	3.9	45.0	20.9	9.1	4.2
3	1.59	50.8	22.0	8.4	4.6	51.1	22.4	8.8	5.0
4	1.44	63.5	28.3	11.3	4.8	63.9	28.9	11.9	5.4
5	1.26	50.1	34.0	9.3	nd	50.7	34.6	10.0	nd
6	1.18	68.2	32.9	13.9	5.3	68.7	33.6	14.7	6.0

6.3 100 h @ 350°C

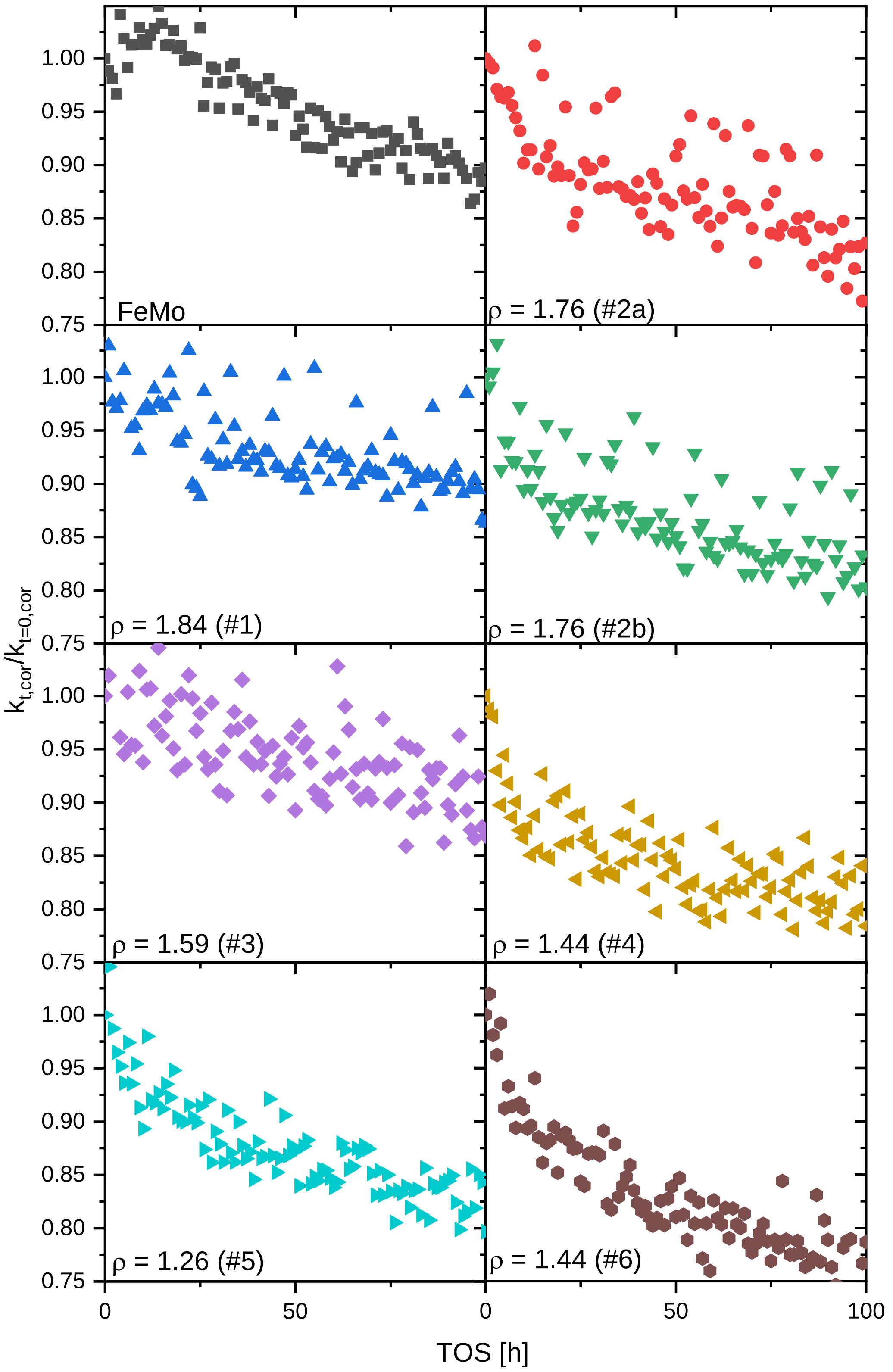

Figure S15: Reversible byproduct corrected observed activity normalized w.r.t. initial rate constant ($k_{t,cor}/k_{t=0,cor}$) at 350°C, 300 NmL/min, 5 vol.% MeOH, 10 vol.% O_2 in N_2.

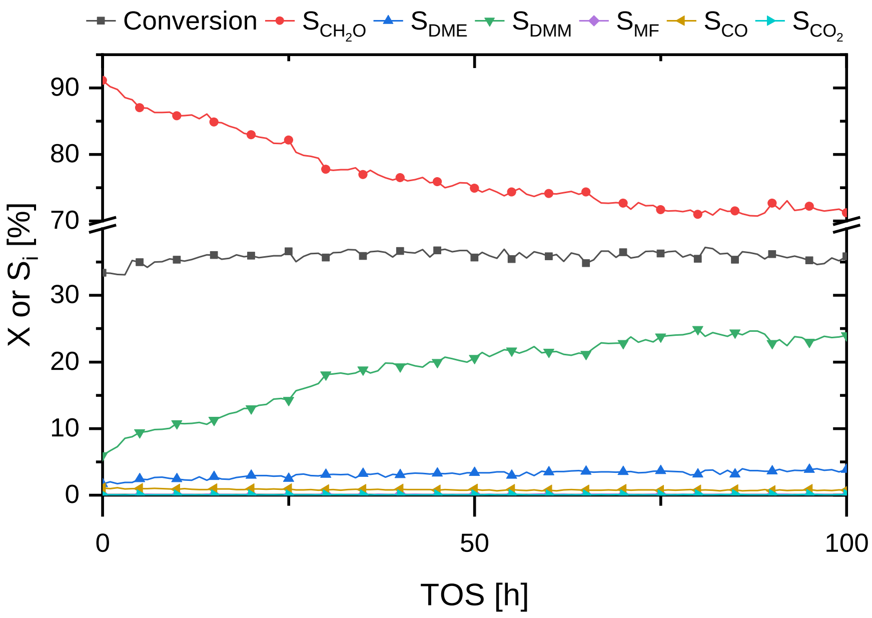

Figure S16: Specific product selectivities and conversion during time on stream for a single FeMo pellet (100 mg) at 350°C, 300 NmL/min, 5 vol.% MeOH, 10 vol.% O_2 in N_2.

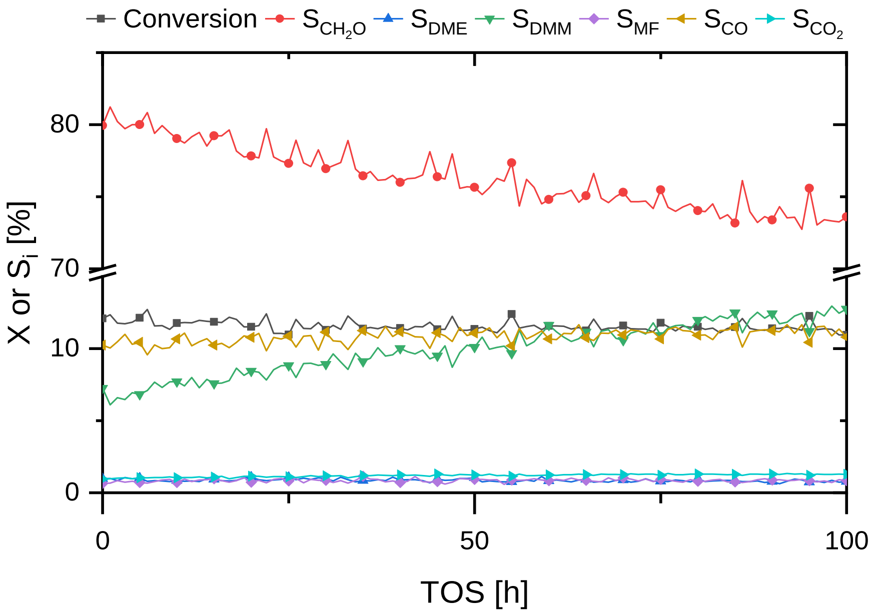

Figure S17: Specific product selectivities and conversion during time on stream for a single ρ = 1.84 g/cm^3 (#1) pellet (104 mg) at 350°C, 300 NmL/min, 5 vol.% MeOH, 10 vol.% O_2 in N_2.

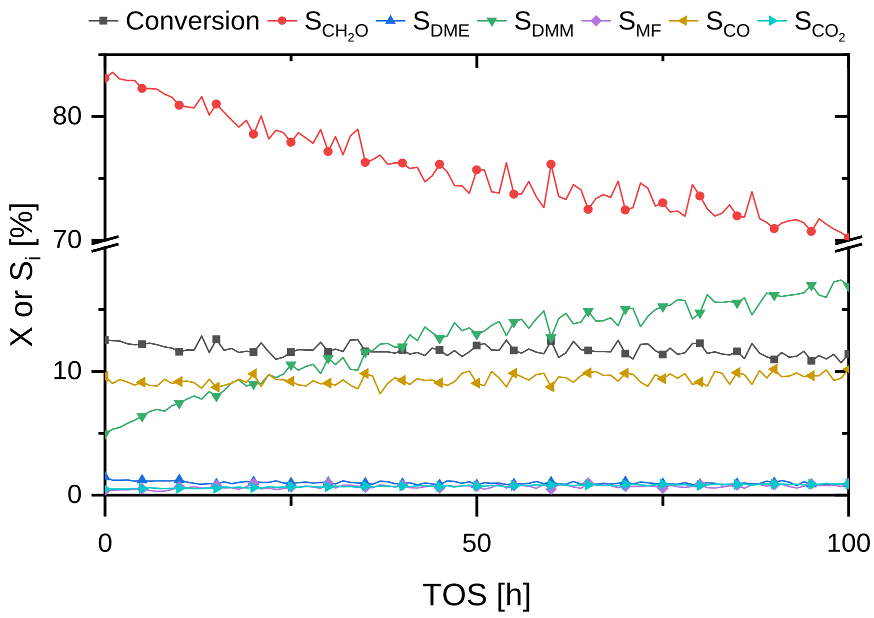

Figure S18: Specific product selectivities and conversion during time on stream for a single ρ = 1.76 g/cm^3 (#2a) pellet (97.2 mg) at 350°C, 300 NmL/min, 5 vol.% MeOH, 10 vol.% O_2 in N_2.

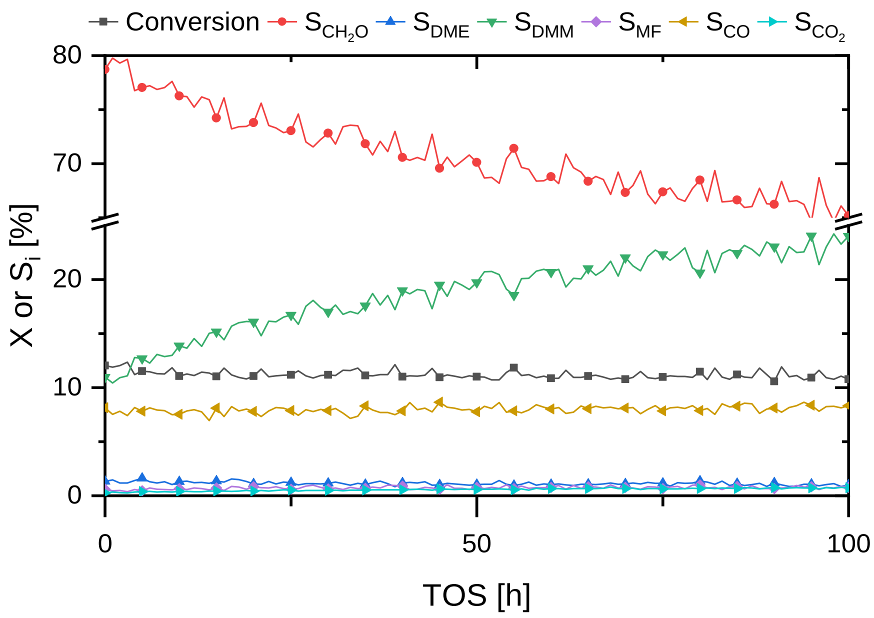

Figure S19: Specific product selectivities and conversion during time on stream for a single ρ = 1.76 g/cm^3 (#2b) pellet (102 mg) at 350°C, 300 NmL/min, 5 vol.% MeOH, 10 vol.% O_2 in N_2.

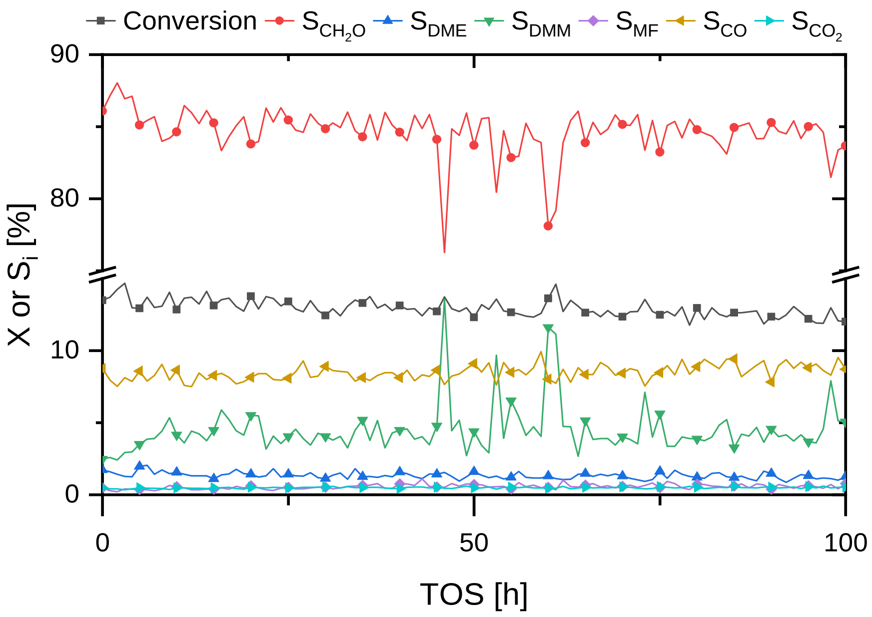

Figure S20: Specific product selectivities and conversion during time on stream for a single ρ = 1.59 g/cm³ (#3) pellet (92.8 mg) at 350°C, 300 NmL/min, 5 vol.% MeOH, 10 vol.% O_2 in N_2.

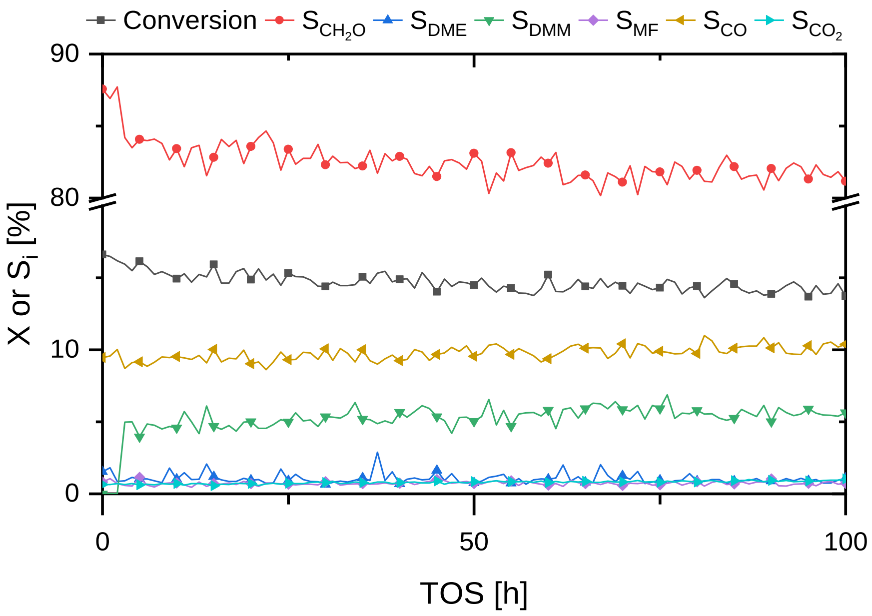

Figure S21: Specific product selectivities and conversion during time on stream for a single ρ = 1.44 g/cm³ (#4) pellet (80.5 mg) at 350°C, 300 NmL/min, 5 vol.% MeOH, 10 vol.% O_2 in N_2.

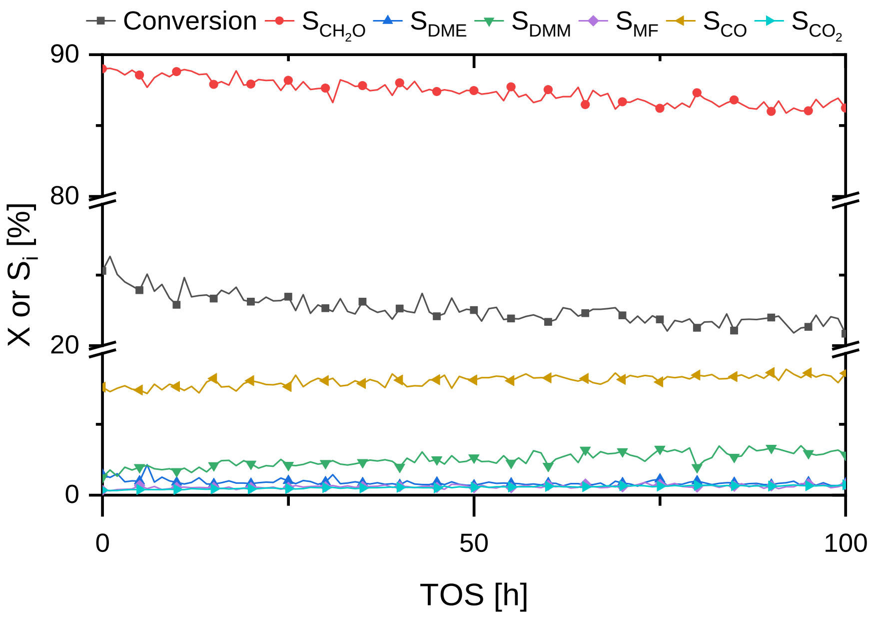

Figure S22: Specific product selectivities and conversion during time on stream for a single ρ = 1.26 g/cm³ (#5) pellet (72.2 mg) at 350°C, 300 NmL/min, 5 vol.% MeOH, 10 vol.% O_2 in N_2.

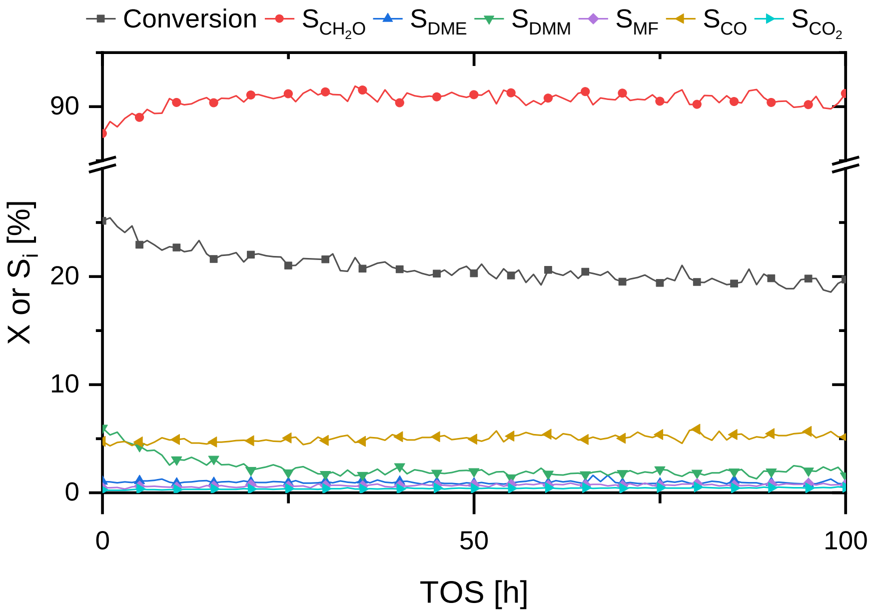

Figure S23: Specific product selectivities and conversion during time on stream for a single ρ = 1.18 g/cm³ (#6) pellet (59.9 mg) at 350°C, 300 NmL/min, 5 vol.% MeOH, 10 vol.% O_2 in N_2.

7 References

[1] F. Kapteijn and J. A. Moulijn, "Laboratory Catalytic Reactors: Aspects of Catalyst Testing," in *Handbook of Heterogeneous Catalysis*, 2nd ed., G. Ertl, H. Knözinger, F. Schüth, and J. Weitkamp, Eds. Weinheim: Wiley-VCH Verlag GmbH & Co. KGaA, 2008, pp. 2019–2045.

[2] R. J. Berger, J.- Perez-Ramirez, F. Kapteijn, and J. A. Moulijn, "Catalyst performance testing: the influence of catalyst bed dilution on the conversion observed," *Chem. Eng. J.*, vol. 90, pp. 173–183, 2002.

[3] H. S. Fogler, *Elements of Chemical Reaction Engineering*, 5th ed. Upper Saddle River, NJ, USA: Prentice Hall, 2016.

[4] D. Kunii and O. Levenspiel, "A General Equation for the Heat-Transfer Coefficient at Wall Surfaces of Gas/Solid Contactors," *Ind. Eng. Chem. Res.*, vol. 30, no. 1, pp. 136–141, 1991.

[5] K. V. Raun *et al.*, "Modeling of the molybdenum loss in iron molybdate catalyst pellets for selective oxidation of methanol to formaldehyde," *Chem. Eng. J.*, vol. 361, no. October 2018, pp. 1285–1295, Apr. 2019.